

# Effects of Al(OH)O nanoparticle agglomerate size in epoxy resin on tension, bending, and fracture properties

Maximilian Jux  · Benedikt Finke ·  
Thorsten Mahrholz · Michael Sinapius ·  
Arno Kwade · Carsten Schilde

Received: 31 August 2016 / Accepted: 16 March 2017 / Published online: 8 April 2017  
© Springer Science+Business Media Dordrecht 2017

**Abstract** Several epoxy Al(OH)O (boehmite) dispersions in an epoxy resin are produced in a kneader to study the mechanistic correlation between the nanoparticle size and mechanical properties of the prepared nanocomposites. The agglomerate size is set by a targeted variation in solid content and temperature during dispersion, resulting in a different level of stress intensity and thus a different final agglomerate size during the process. The suspension viscosity was used for the estimation of stress energy in laminar shear flow. Agglomerate size measurements are executed via dynamic light scattering to ensure the quality of the produced dispersions. Furthermore, various nanocomposite samples are prepared for three-point bending, tension, and fracture toughness tests. The screening of the size effect is executed with at least seven samples per agglomerate size and test method. The variation of solid content is found to be a reliable method to adjust the agglomerate size between 138–354 nm during dispersion. The size effect on the Young's modulus and the

critical stress intensity is only marginal. Nevertheless, there is a statistically relevant trend showing a linear increase with a decrease in agglomerate size. In contrast, the size effect is more dominant to the sample's strain and stress at failure. Unlike microscaled agglomerates or particles, which lead to embrittlement of the composite material, nanoscaled agglomerates or particles cause the composite elongation to be nearly of the same level as the base material. The observed effect is valid for agglomerate sizes between 138–354 nm and a particle mass fraction of 10 wt%.

**Keywords** Boehmite · Nanoparticles · Epoxy resin · Dispersing · Viscosity · Fracture toughness · Nanoscale mechanics · Nanocomposites

## Introduction

For more than 40 years, researchers have been observing the influence of solid particles in epoxy resin on the mechanical properties of composite materials (Radford 1971; Lange and Radford 1971). Epoxy resins possess outstanding mechanical properties and are highly resistant to chemicals, which enable numerous applications such as weight-bearing structures, surface coatings, and adhesives, in a broad range of industries, e.g., aerospace, automotive, and construction industries. Thus, epoxy resin is an established engineering material and is often used as a preferred resin component in fiber-reinforced structures. Particle-modified epoxy resins are still generating considerable research interest. A relevant

---

M. Jux (✉) · M. Sinapius  
Institute of Adaptic and Functional Integration (IAF), TU  
Braunschweig, Langer Kamp 6, 38106 Braunschweig, Germany  
e-mail: maximilian.jux@dlr.de

B. Finke · A. Kwade · C. Schilde  
Institute for Particle Technology (IPAT), TU Braunschweig,  
Volkmaroder Str. 5, 38104 Braunschweig, Germany

T. Mahrholz  
Institute of Composite Structures and Adaptive Systems (FA),  
DLR Braunschweig, Lilienthalplatz 7-9, 38108 Braunschweig,  
Germany

research area is the size effect of primary particles and agglomerates on the mechanical properties of particle-reinforced composites (Jamaati et al. 2014; Fu et al. 2008). However, few researchers have addressed the problem of connecting size analysis results with mechanical test results. In the majority of cases, the filler size is simply taken from the manufacturer and supported by an additional figure from a scanning electron microscope. Measurements with the microscope, however, are usually based on surface pictures of cured samples, without knowing the true size of the filler material and on a relatively small number of particles or agglomerates. Another method is to use optical procedures like dynamic light scattering techniques (Nolte et al. 2012). The size effect of boehmite agglomerates on the mechanical properties of epoxy resins has not been studied yet. Considering the question of size effects in general, the research on boehmite may provide an opportunity to further generalize the results that are reported in the literature. It is expected that boehmite has a significant impact on the mechanical properties of epoxy resin, in particular on the fracture toughness under mode-I loading and under tensional loading. The current state of research is summarized below, including the results of several studies, which deal with size effects of different filler materials on the mechanical properties of composite materials.

Based on test results from Radford (1971), Fu et al. (2008) stated that the tensile modulus of epoxy/aluminum resin composites is not significantly affected for primary particle sizes between 1  $\mu\text{m}$  (6.9 GPa) and 12  $\mu\text{m}$  (6.6 GPa) at a constant volume fraction of 29.5 vol%. Furthermore, the fracture energy was investigated with the same material and average particle sizes. According to these results, the fracture energy reached the greatest values for the composites with the largest primary particle size of 12  $\mu\text{m}$ . Jamaati et al. (2014) compared the effects of microparticles and nanoparticles on the microstructure and the mechanical properties of steel-based composites. They reported that higher particle sizes and higher aspect ratios were more susceptible to particle breaking. Hall et al. (1994) measured an increase of about 26% in tensile and 13% in yield strength in aluminum/silica composites for primary particle sizes between 2 and 20  $\mu\text{m}$  at a volume fraction of 20 vol%. Furthermore, Nakamura et al. (1992) identified an increase in tensile strength and absorbed impact energy in epoxy/silica composites for primary particle sizes in a range from 2 to 42  $\mu\text{m}$  for a mass fraction of

64 wt%. In addition, they discussed the influence of primary particle size on agglomeration. They found that an increasing particle size leads to a more irregular shape of the agglomerates and assumed that the irregular shape may cause lowered resistance against cracking. Singh et al. (2002) examined the fracture toughness of polyester/aluminum composites for the primary particle sizes 100 nm, 3.5  $\mu\text{m}$ , and 20  $\mu\text{m}$  at volume fractions between 0 and 5%. They found that primary particle size and volume fraction have a strong impact on the fracture toughness and they measured an increase in fracture toughness of 5% for 20  $\mu\text{m}$ , 20% for 3.5  $\mu\text{m}$ , and 32% for 100 nm compared to the unfilled polyester resin at a volume fraction of 1%. Furthermore, they found that the volume fraction influences the agglomeration, and that nanoparticles are more inclined to agglomeration than microparticles. Al-Turaif (2010) observed the effect of nano  $\text{TiO}_2$  on the mechanical properties of epoxy resin for primary particle sizes of 17, 50, and 220 nm at volume fractions between 0 and 10%. The results showed that the investigated mechanical properties including tensile stress, elongation at break, toughness, the Young's modulus, flexural stress, abrasion rate, and pull-off strength increase with decreasing particle sizes. Some of the experimental test results in the literature indicate that the particle size has no significant impact on the elastic modulus (Radford 1971, Fu et al. 2008). However, considering the notch effect and stress concentrations caused by the particles, it is anticipated that the particle size has a decisive effect on the fracture behavior under tensional loading.

The fracture behavior is generally an important aspect concerning the mechanical properties of composite materials. Particularly, the fracture toughness and thus the particle-induced toughening mechanisms are crucial to comprehend the fracture behavior of composite materials. There are two main categories of toughening mechanisms. These are on-plane mechanisms like crack pinning or crack deflection and off-plane mechanisms like debonding and plastic void growth. In particular, the works of Lange (1970), Lange and Radford (1971), Evans (1972), Green et al. (1979), Kinloch et al. (2005, 1985, Kinloch and Williams 1980), and Wetzel et al. (2006) made major contributions concerning the research on toughening mechanisms. The toughening mechanisms taking place depend on the filler materials size and on the strength of the interaction between additive and matrix. The mechanical properties of the filler material are important, too. Especially in the submicron range, the particle strength

increases with decreasing particle size (Rumpf 1959) and can therefore endure higher stresses before yielding. For a strong particle-matrix interaction and a high stiffness of the particle, most likely on-plane mechanisms occur. However, due to the fact that the particles are significantly smaller than the crack, it is questionable if these mechanisms are present on the nanoscale. In contrast, weak particle-matrix interactions most certainly lead to off-plane mechanisms. Next to the toughening mechanisms, other effects like interfacial stress transfer and local changes in cross-link density may also be affected by the particle size and thus influence the mechanical properties. Furthermore, it is assumed that smaller particles or agglomerates do not corrupt the matrix polymer network as their spatial extent is smaller and therefore causes less distortion of the network.

This paper presents a detailed description of manufacturing boehmite/epoxy resin dispersions, along with results of size analysis and mechanical tests. Several methods exist for dispersing nanoparticles in resin. These utilize several stress mechanisms such as stressing between surfaces, stressing in laminar shear flow, and ultrasonication. Stressing between surfaces can be performed in stirred media mills delivering the highest fineness. Ultrasonication is a widely applied method for the production of nanoparticles in lab scale quantities. Both methods are limited to low solid content, since the viscosity of the material needs to be kept low in order to achieve good dispersion results (Bittmann et al. 2009; Knieke et al. 2010). Additionally, the solid content of nanoparticles has a strong influence on the suspension viscosity. In this study, a kneader was chosen for the production of nanocomposite suspensions, as laminar shear flow is the main stress mechanism acting in this device. The samples for the mechanical tests were fabricated with the characterized dispersions using a combination of casting and milling processes. Selected mechanical properties like tensile, bending, and fracture tests were examined for average agglomerate sizes between 140 to 350 nm at a constant mass fraction of 10 wt%. Considering the boehmite agglomerates in this study, it is expected that the smaller the agglomerates are, the stiffer and stronger they will be, since the average strength of interparticle interactions will necessarily increase as agglomerate size decreases through repeated disruption of the weakest points in the system during the dispersion process. Thus, a decreasing agglomerate size will simultaneously lead to a change in the mechanical properties.

The authors, when speaking of a size effect, address both the effect of the spatial extent of the agglomerates and synergetic effects like the change in the agglomerates stiffness and the specific surface area.

## Materials and methods

### Materials

The dispersions and the samples were produced with cubic boehmite (DISPERAL HP14, SASOL, Germany) with an average agglomerate size of 25  $\mu\text{m}$  and a primary particle size of 14 nm according to the manufacturer. SASOL applies the *On-Purpose Process* (Torno 2008) for the production of the particles. Al—metal, higher alcohols, and hydrogen are used for this process. The particles are dispersed in bisphenol-A-diglycidylether (DGEBA, Araldite® LY 556, Huntsman). The epoxy resin is along with methyltetrahydrophthalic acid anhydride (MTHPA, Aradur® HY 917, Huntsman) and methylimidazole accelerator (Accelerator DY 070, HUNTSMAN, Germany) a hot curing matrix system. The mix ratio amounts to 100:90:1 parts per weight. Boehmite particles were dispersed in DGEBA epoxy resin at varying solid contents and subsequently diluted with the bisphenol-A epoxy resin to produce a suspension with a solid content of 30 wt%. This master suspension was stored at  $-20\text{ }^{\circ}\text{C}$ , which prevents an agglomeration or aggregation and cross-linking of the particles with the epoxy resin. The presence of a nanoparticle or agglomerate represents an obstacle to cross-linking and will ensure that the cross-link density near the particle surface is changed compared to the neat resin. Boehmite has a crystalline structure with functional OH groups on the surface. Since the size effect is studied, it should be mentioned that the exposed surface area of boehmite and thus the OH groups increase with reduced agglomerate sizes. The OH groups may bind or deactivate resin components or alter the curing behavior due to other chemical reactions (Exner et al. 2012).

### Dispersing

In order to adjust the average size of the boehmite particles within the dispersion by varying particle content and temperature during dispersing, experiments were conducted in a high-performance laboratory

kneader HKD-T0.6 (IKA, Germany). To enable the production of suspensions with a defined agglomerate size, a preliminary exploratory experiment was conducted, in which the particle content was gradually increased after a steady final agglomerate particle size was reached. Steadiness was usually reached after 120–150 min, which is why 180 min was chosen as the standard dispersing time in this experiment. It must be noted that the achievable stress intensities in laminar shear flow do not suffice to induce breakage of primary particles; therefore, only the agglomerate size is altered in this process. Similar to the experiments conducted by Nolte et al. (2010), this experiment provides information about the solid content, which is necessary to reach a desired final agglomerate size. The size measurements were conducted with a Nanophox (Sympatec, Germany) following a method described in Nolte et al. (2012) where the suspension is diluted with a mixture of a solvent and stabilizing agent, which resulted in a sample with sufficient particle mobility to enable the measurement via dynamic light scattering. Since the result of a dynamic light scattering measurement is based on the estimation of the rate of diffusion, the agglomerate size is assessed with this method.

Dilution was performed with a mixture of ethanol, water (80:20 parts per volume), and the stabilizing agent Disperbyk 1142 (Byk) to a particle solids content of 0.06 wt% at a stabilizer ratio of  $50 \frac{\text{g}_{\text{stabilizer}}}{\text{g}_{\text{particle}}}$ . While establishing this method, the stability of the particle size was tested by repeated measurements for a period of 6 h. Further proof of the stability was gained by scanning the transmission and back-scattering profile of a sample with a Turbiscan (Formulation, France) that confirmed the absence of re-agglomeration and sedimentation. A change in particle size, as discussed by Nolte et al. (2012), can therefore only happen during the wetting of the particles by the stabilizing agent at the start of the solution. The polar solvent mixture ensures a slow solvation ( $< 2 \text{ mg/min}$ ) of the epoxy matrix, and the high stabilizer ratio ensures a good availability of stabilizer molecules which minimizes a potential initial re-agglomeration of the particles. This guarantees the comparability of the particle sizes measured in this study. For the comparison of the obtained suspensions, the  $x_{10,3}$ ,  $x_{50,3}$ , and  $x_{90,3}$  values were considered. They indicate the particle size when the volume weighted (Index 3) cumulative particle size distribution reaches the value of 10, 50, or 90%, respectively.

The suspensions for the test specimen were prepared based on the knowledge about the correlation of solid content and the resulting final agglomerate size. The batches were then produced with formulation and process parameters that allowed a wide range of agglomerate sizes. The experiments were conducted at solid contents of 40, 32, and 25 wt% at a temperature of 20 °C. In order to produce a suspension with larger agglomerate sizes an additional experiment was conducted at 50 °C at the minimum required solid content.

For the estimation of the stress intensity according to Rumpf and Raasch, viscosity was measured in a rotatory rheometer (Kinexus, Malvern) with a plate-plate arrangement (20 mm diameter, 0.5 mm gap width, shear rate  $50 \text{ s}^{-1}$ ). In the case that the viscosity exceeded the measurement range of the rheometer, samples were diluted and values with high solid contents were extrapolated by an exponential function.

#### *Specimen preparation*

Initially, the suspension was diluted with neat epoxy resin by carefully blending the components with a vacuum centrifugal mixer (PASTE MIXER PDM-300V, DAE WHA TECH) at rotational speeds of up to 1350 rpm. The process was executed at varying rotational speeds in order to increase the mixing effect and under a vacuum for a first reduction of air pockets. To obtain a homogeneous result, the blending was performed twice in a row for 90 s. The hardener and the accelerator were blended with the diluted suspension after a visual control indicated a homogeneous blend of suspension and neat epoxy resin. Before further processing, the particle-epoxy resin matrix system was filtered with a fine sieve (mesh size approximately 190  $\mu\text{m}$ ) to eliminate foreign objects from the dispersion process. It was then degassed for 10 min at a pressure of 0.2 mbar to eliminate foreign air. Subsequently, the material was cast in a preheated (80 °C) casting tool (depending on the test method, a size of nearly DIN A4 with thicknesses between 2 and 5 mm) and cured for 4 h at 80 °C for gelation and 4 h at 120 °C for post-curing. The casting tool is made of stainless steel and to provide an easy release a water-based mold release system (WaterWorks Aerospace Release) was used. Tension specimens were produced according to the standard DIN EN ISO 527-2 sample type 1B with a thickness of 2 mm, bending specimens were produced according

to DIN EN ISO 178 with geometry of  $80 \times 10 \times 2$  mm, and fracture toughness specimens were produced according to ISO 13586 with a thickness of 5 mm. The edges of the samples were polished slightly with fine abrasive paper (600 grain size) to remove any influence of microcracks produced during the milling process.

### Mechanical testing

For a statistical coverage of the test results, a minimum of seven tensile samples, ten bending samples, and ten fracture toughness samples were measured. The test specimens were conditioned at a temperature of 23 °C and a humidity of 51% for at least 2 days. Afterwards, the mechanical tests were performed on a static testing machine type Z005 from Zwick/Roell with a maximum test load of 5 kN.

### Tensile test

For the tensile test, the stress/strain curves were recorded with a test speed of 1 mm/min and a minor load of 5 N. The tension modulus is calculated by using the increase of the secant:

$$E_t = \frac{\sigma_2 - \sigma_1}{\varepsilon_2 - \varepsilon_1} \quad (1)$$

$E_t$  is the tension modulus in MPa,  $\sigma_1$  is the stress in MPa measured at a strain of  $\varepsilon_1 = 0.05\%$ , and  $\sigma_2$  is the stress in MPa measured at a strain of  $\varepsilon_2 = 0.25\%$  (DIN EN ISO 527-1). No value is specified for the standard deviation in DIN EN ISO 527. The standard deviation of the tensile test was specified with a limit of 3%, oriented on the obtained test results.

### Bending test

According to DIN EN ISO 178 (three-point bending), the test speed was set to 2 mm/min and a minor load of 5 N. The bending modulus is calculated analogously to the tensile modulus, but the strain values are replaced with the deflection values. The test standard for the bending test does not define a standard deviation. Due to the test results, it was determined that the standard deviation must not exceed 5%.

### Fracture toughness test

Fracture toughness tests were performed with a test speed of 10 mm/min. For the evaluation of the fracture toughness, the critical energy release rate  $G$  and the critical stress intensity factor were used. The energy release rate is “the change in the external work  $\delta U_{\text{ext}}$  and strain energy  $\delta U_S$  of a deformed body due to enlargement of the cracked area  $\delta A$ ” (ISO 13586), expressed in  $\text{J/m}^2$ :

$$G = \frac{\delta U_{\text{ext}}}{\delta A} - \frac{\delta U_S}{\delta A} \quad (2)$$

The critical energy release rate corresponds to the value of the energy release rate when the crack starts to grow in a precracked specimen. The critical stress intensity factor  $K_{1C}$ , expressed in  $\text{Pa} \times \sqrt{\text{m}}$ , is the limiting value depending on the stress perpendicular to the crack area and the distance from the crack tip when the crack starts to propagate. Furthermore, it is related to the critical energy release rate by the following equation:

$$G_{1C} = \frac{K_{1C}^2}{E} \quad (3)$$

$E$  is the modulus of elasticity, calculated with the help of the tensile modulus. The samples for the fracture toughness tests were precracked with a crack length ranging from 7 to 13 mm. It is imperative that close attention must be paid to the statistic deviation of the test results, since the deviation must not exceed 12% (under the terms of ISO 1358).

### Rheological characterization

Shear viscosity was measured in a rotatory viscometer (Kinexus, Malvern) with a plate to plate geometry for diluted samples from the suspension with an agglomerate size of 140 nm. Each sample was tested three times at temperatures of 20 and 50 °C. The samples had to be diluted with neat epoxy in order to allow the examination via rotatory viscosimetry, since samples above 20 wt% present poor wetting behavior to the rheometer plate at 20 °C, which causes wall slip and yields in unsteady measurements. After the dilution step, the agglomerate size was measured again to dismiss potential instability of the sample.

## Results and discussion

### Dispersing

#### Exploratory experiment

During the exploratory experiment, the solid content was increased every 180 min, when the agglomerate size had reached a final value. Figure 1 illustrates the dependency of final agglomerate size, reached during the dispersion experiments on the solid content. Both the results from the exploratory fed batch experiment and the experiments performed for the production of the material for the test specimens show that the final agglomerate size decreases with rising solid content. The reason for this is an increased stressing of the agglomerates in the laminar shear flow, acting in the kneader due to the viscosity increase of the suspension or rather the increase in shear rate, respectively, which is caused by the addition of particles to the suspension. This behavior is in accordance with earlier work with similar material combinations (Nolte et al. 2010). The subsequent production of the material for the test specimen leads to agglomerate sizes similar to those expected from the exploratory results (compare Fig. 1). Dispersing at elevated temperatures and resulting lower viscosities causes a higher final agglomerate size. Consequently, high agglomerate sizes can be achieved despite working with high solid content.

The shear stress  $\tau$  acting on a spherical particle can be estimated by (Eq. 4) (Rumpf and Raasch 1962) and is considered to be proportional to the stress intensity acting on the particles (Schilde et al. 2010). The shear rate  $\gamma$  can be calculated by using the viscosity of the fluid and a model proposed by Reichert and Ruhmling (1976) (Eq. 5). With rising solid content, the viscosity  $\eta$  of the suspension increases, which gives rise to an increased stress intensity  $SI$  (Nolte et al. 2010).

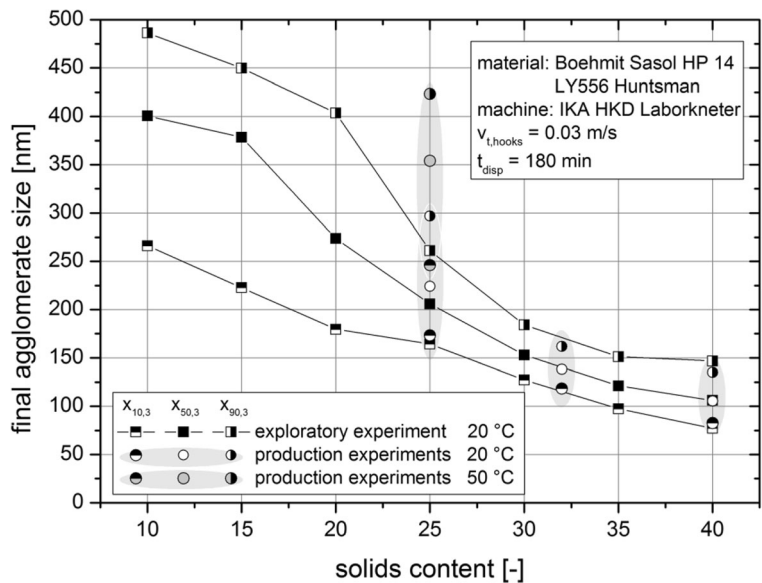
$$SI \propto \tau = 2.5 \times \gamma \times \eta \tag{4}$$

$$\gamma = \frac{\pi \times n \times (r_{\text{chamber}} + r_{\text{hook}})}{h_{\text{gap}}} \tag{5}$$

The shear viscosity at the individual solids contents was characterized via rotational viscosimetry. There exist numerous equations to model the viscosity of suspensions. While most deal with dilute suspensions of microscale particles, some cover particles in the sub-micron range. Yet, no model known to the authors sufficiently describes the behavior presented by the system that is discussed in this study. The best approximation of the viscosity as a function of the solid content  $c_m$  is obtained by the exponential equation:

$$\eta(c_m) = A \times e^{\frac{c_m}{B}} + C \tag{6}$$

**Fig. 1** Dependency of the agglomerate size on the solid content for exploratory and production experiments



with the set of parameters A, B, and C. The approximation was performed weighted by the viscosity value. This is due to the rise of distorting effects like air bubble trapping in the suspension sample and wall slip during the measurement when viscosity increases. Minimized standard errors for the individual values were found for a rather strong weighting factor of  $\omega_i = \frac{1}{\eta_i^2}$  with  $\omega$  being the weighting factor of the Levensberg-Marquardt algorithm for the data approximation. This causes an increasing neglecting of data points with high viscosity values. The search for a physically based model for the viscosity of nanoparticulate suspensions with respect to disperse properties and surface effects is the focus of ongoing research that is driven by the authors parallel to this study. A more physically justified approach of the modeling must therefore be deferred to a following publication.

As can be seen in Fig. 2, (Eq. 6) provides a very good fit for the data points that were obtained for particle contents from 1 to 17.5 wt%. After that, the approximated viscosity rises faster as the data points. The confidence intervals constituted by the standard errors of the individual approximation parameters are represented by a gray belt. It depicts the uncertainties of the extrapolation despite the good fit ( $R^2 = 0.989$ ). The standard errors of the data fit are displayed in Table 1.

Since a characterization of the suspension viscosity at solid contents higher than  $c_m = 0.2$  is not possible via rotatory viscosimetry as the torque exceeds the limits of

common rheometers, the results need to be extrapolated according to (Eq. 6), in order to obtain values for formulations used for dispersing. These values were then incorporated into the estimation of maximum stress intensities acting during the dispersing processes according to (Eq. 4) (Rumpf and Raasch 1962). The results are displayed in Fig. 3, showing the dependency of the final agglomerate size of the dispersion on the maximum stress intensity of the dispersion experiments in a kneader. The results from the exploratory fed batch experiment and the experiments performed for the production of the material for the test specimens are compared in Fig. 3. Error bars display the uncertainties of the calculated stress intensities resulting from the approximation of the viscosity data. Both the exploratory experiment and the subsequent production of the sample material can be described by the exponential function, which is plotted as a solid black line. The approximation results in a  $R^2$  value of 0.941. Deviations may arise from errors due to the demanding task of measuring the viscosity of highly filled resin suspensions and the assumption that the temperature in the gap between kneading hooks and chamber wall equals the coolant temperature. The immense energy dissipation during dispersing may increase the temperature of the material. Yet, the final agglomerate size is determined by the highest stress intensities that are expected to act in close proximity to the chamber wall, where the temperature is closest to that of the coolant.

**Fig. 2** Approximation and extrapolation of experimental data as a function of solid content

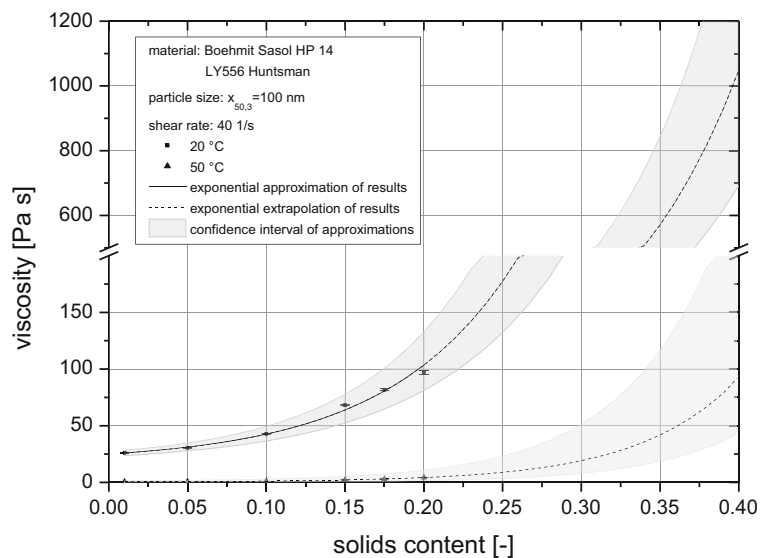


**Table 1** Parameters and standard errors for the approximation of the suspension viscosity over the solid content

Temperature of measurement	20 °C		50 °C	
Parameter	Value	Standard error	Value	Standard error
A	7.116	0.974	0.159	0.035
B	0.080	0.005	0.063	0.004
C	17.898	1.202	0.440	0.121

### Particle size distribution of the dispersions and the cured composites

The reproducibility of the process was evaluated by repeating the experiment 14 times. It resulted in a standard deviation of below 10 nm for all agglomerate size values along the distribution, which corresponds to the deviation of the measurement accuracy. The mean of the 14 agglomerate size distributions is plotted in Fig. 4 with the standard deviation of the agglomerate size.

The evaluation of the cured composites agglomerate distribution was realized with SEM pictures of cryogenic fracture samples. These images help in estimating whether the particle distribution is homogeneous and if the particles re-agglomerate during the mixing and

curing process. It should be pointed out that the primary particle size of boehmite amounts to 14 nm. Thus, it can be expected that for size distributions ranging from 140 to 400 nm, agglomerates have a high likelihood of being found. Figure 5 shows a SEM picture of a cured boehmite-epoxy composite fracture sample. It can be assumed that most of the brighter structures in the image are particles, and that the darker gaps are areas of debonded particles or agglomerates. As anticipated, a high proportion of the particles were agglomerated, but primary particles could also be found. The distribution of the agglomerates appears homogeneous, and the size distribution also corresponds to the size measurement via dynamic light scattering. Nevertheless, it is important to mention that SEM pictures are not a statistically reliable source for measuring size distribution. These images only depict small local areas of the overall sample, and the real size of the agglomerates beneath the surface is unknown.

### Mechanical characterization

The purpose of this work was to investigate the size effects of boehmite particles on the mechanical properties of epoxy nanocomposites. Existing research has shown that the properties are only slightly improved with decreasing particle sizes (Radford 1971; Lange

**Fig. 3** Dependency of the final agglomerate size on the stress intensity calculated by (Eq. 4) (Rumpf and Raasch 1962) based on the viscosity of the suspension

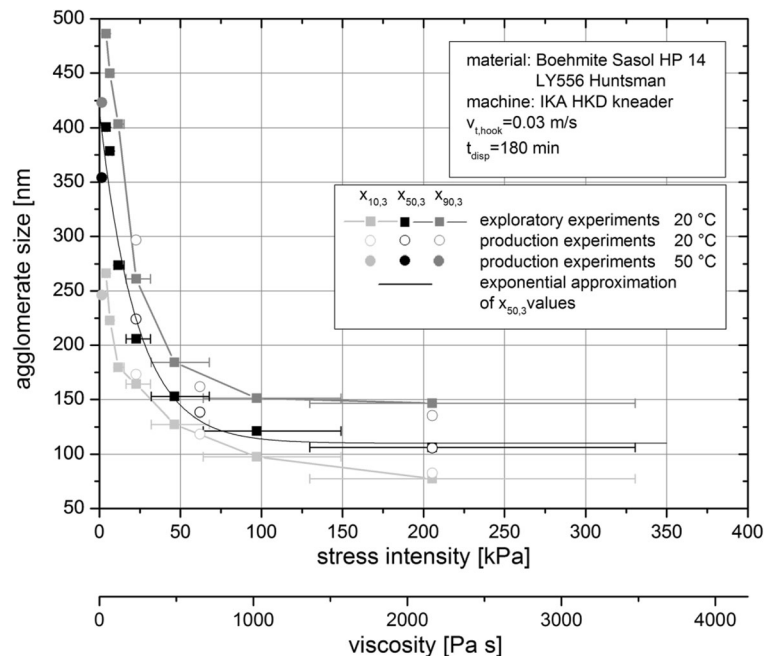
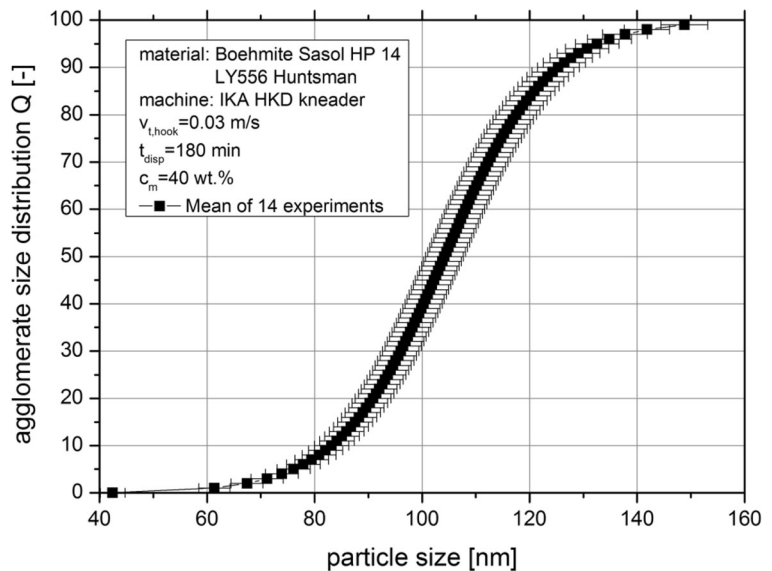


**Fig. 4** Mean agglomerate size distribution of dispersing experiments under the same process conditions



and Radford 1971; Fu et al. 2008). Significant increases were measured mainly for microscale particles with sizes down to a minimum particle diameter of 2  $\mu\text{m}$  (Hall et al. 1994; Nakamura et al. 1992). The average values of all mechanical test results measured during this study are summarized in Table 2. The agglomerate sizes given in Table 2 correspond to median agglomerate size values  $x_{50}$  determined with the volume-based size distribution measurement, described in Nolte et al. (2012).

Figure 6 shows the percentage change in mechanical properties compared to the unfilled epoxy resin system depending on the agglomerate size at a constant mass fraction of 10%. The mechanical properties are measured at the average agglomerate sizes of 138, 251, and 354 nm. Figure 6a shows the influence of the agglomerate size on Young's modulus for tension and bending tests. The standard deviations for the tensile tests (0–1%) are smaller than those of the bending tests (1–2%). This results from the more precise measurement technology of the tension test method and from the different type of loading concerning the test methods. For both test methods, the results increase nearly linearly with decreasing particle size with a marginal change of about 2–3%. Compared to the neat epoxy resin, there is a maximum increase of 13% for the bending modulus and 16.5% for the tension modulus at an agglomerate size of 138 nm. These results are in accordance with existing research (Radford 1971; Lange and Radford 1971; Fu et al. 2008). Looking at different material

models and rules of mixtures, the two main parameters having an influence on the elastic modulus of the composite material are the volume fraction and the elastic modulus of the individual components. Due to the fact that agglomerates gain stiffness with a size reduction, the increase in the elastic modulus of the composite might not be only caused by the smaller spatial extend of the particles but also by their increased stiffness. Additionally, the interfacial stress transfer should be considered. In particular, as agglomerate size is reduced and more of the surface area of the primary particles becomes accessible, the interfacial stress transfer should increase, due to the fact that there are more interfaces the stress can be transferred through. The maximum tension and bending strain can be seen in Fig. 6b. There is a significant increase in the maximum strain of about 40%

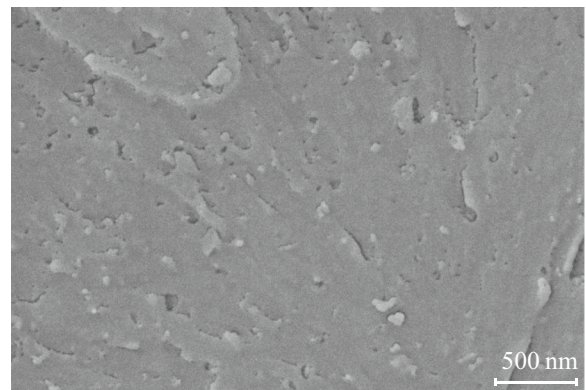


**Fig. 5** SEM picture of 10% boehmite by weight in the epoxy resin

**Table 2** Mechanical test results for tension, bending, and fracture toughness tests at a constant mass fraction of 10 wt%—average values and standard deviations

Agglomerate size (nm)	Tension			Bending			Fracture toughness	
	$E$ (MPa)	$\varepsilon_{\text{ultimate}}$ (%)	$\sigma_{\text{ultimate}}$ (MPa)	$E$ (MPa)	$\varepsilon_{\text{ultimate}}$ (%)	$\sigma_{\text{ultimate}}$ (MPa)	$K_{1C}$ (kPa $\sqrt{\text{m}}$ )	$G_{1C}$ (J/m $^2$ )
Reference	3333 ± 17	5.3 ± 1.0	87.3 ± 1.3	3370 ± 29	6.5 ± 0.1	143.4 ± 0.8	502 ± 11	109 ± 6
138	3884 ± 39	4.3 ± 0.6	88.7 ± 0.9	3810 ± 88	6.2 ± 0.2	148.3 ± 2.8	697 ± 12	181 ± 14
224	3845 ± 34	2.3 ± 0.1	71.2 ± 2.2	3750 ± 62	4.2 ± 0.5	131.2 ± 8.5	686 ± 13	179 ± 14
354	3813 ± 12	2.2 ± 0.1	68.3 ± 1.9	3700 ± 54	3.5 ± 0.5	116.5 ± 10.5	670 ± 26	175 ± 11

for both test methods comparing the composites with an average agglomerate size of 354 and 138 nm. This phenomenon indicates an embrittlement of the composite material with increasing agglomerate size. Larger agglomerates are weak spots and will break earlier producing larger damage zones and thus resulting in a premature failure of the test specimen. The relation between agglomerate size and maximum strain is nearly exponential for agglomerate sizes between 138 to 354 nm. The difference between the results of the tension and bending test might occur because the bending specimens are subjected to a slipping effect between the specimen and the supports if a certain level of loading is reached. The maximum strength displayed in Fig. 6c shows a similar behavior. It can also be described as a significant increase with an improvement above 20% for a comparison between the composites with agglomerate sizes of 138 and 354 nm. At an agglomerate size of 138 nm, the maximum strength even exceeds the neat resin. For the experimental tests under tensional loading, it is expected to find a strong correlation between agglomerate size and stress concentrations around the agglomerates. Thus, a decreasing particle size may lead to a decreased notch effect resulting in an increased strain and strength.

The analysis of the mechanical cracking was executed with compact tension (CT) specimens subjected to fracture toughness tests. The results are shown in Fig. 6d. The standard deviations of the fracture toughness tests do not exceed 12%, which is a criterion for considering the results as valid. Generally, the influence of particle reinforcement is considerably higher on the fracture toughness than on the modulus of elasticity. An improvement of about 40% in the critical stress intensity factor and 70% in the critical energy release rate for a particle size of 138 nm was measured compared to the unfilled epoxy resin. Figure 7 shows a picture of the

fracture surfaces of 7a – neat epoxy in comparison to epoxy with a mass fraction of 10 wt% boehmite and agglomerate sizes of 7b – 354 nm, 7c – 224 nm, and 7d – 138 nm. The pictures were taken from the tested CT specimen close to the initial crack area. The crack direction goes from the right side to the left side of the pictures. The change in mechanical properties caused by particle modification and the change in particle size clearly affects the appearance of the fracture surface, too. The fracture surface of the neat epoxy resin is very smooth compared to the fracture surface of the particle-modified composites. Furthermore, it can be seen that the roughness of the fracture surface increases with decreasing agglomerate sizes. The surface roughness is an indicator for crack deflection. If the surface roughness rises, it is more likely that crack deflection processes occur. The crack deflection process increases the total fracture surface leading to increasing energy absorption. A theory and the associated experiments of crack deflection processes were described and performed by Faber and Evans (1983a, b). Jamaati et al. (2014) guessed that large particles cause a high possibility of particle breaking, leading to an increase in the fracture toughness. In the framework of this study, no hint for agglomerate breaking could be found. It is questionable if broken agglomerates remain in the matrix and if they would look any different from smaller agglomerates that have managed to deflect a passing crack. Another possibility is that an irregular agglomerate fracture results in an increased roughness of the fracture surface. Based on the SEM pictures in Fig. 7, it is estimated that de-bonding takes place, too. Voids in the epoxy resin are an indicator for de-bonding. The de-bonded particles or agglomerates could either remain in the opposite fracture surface or have been fallen out completely during the cracking. The total number of voids is increasing with decreasing particle size. The

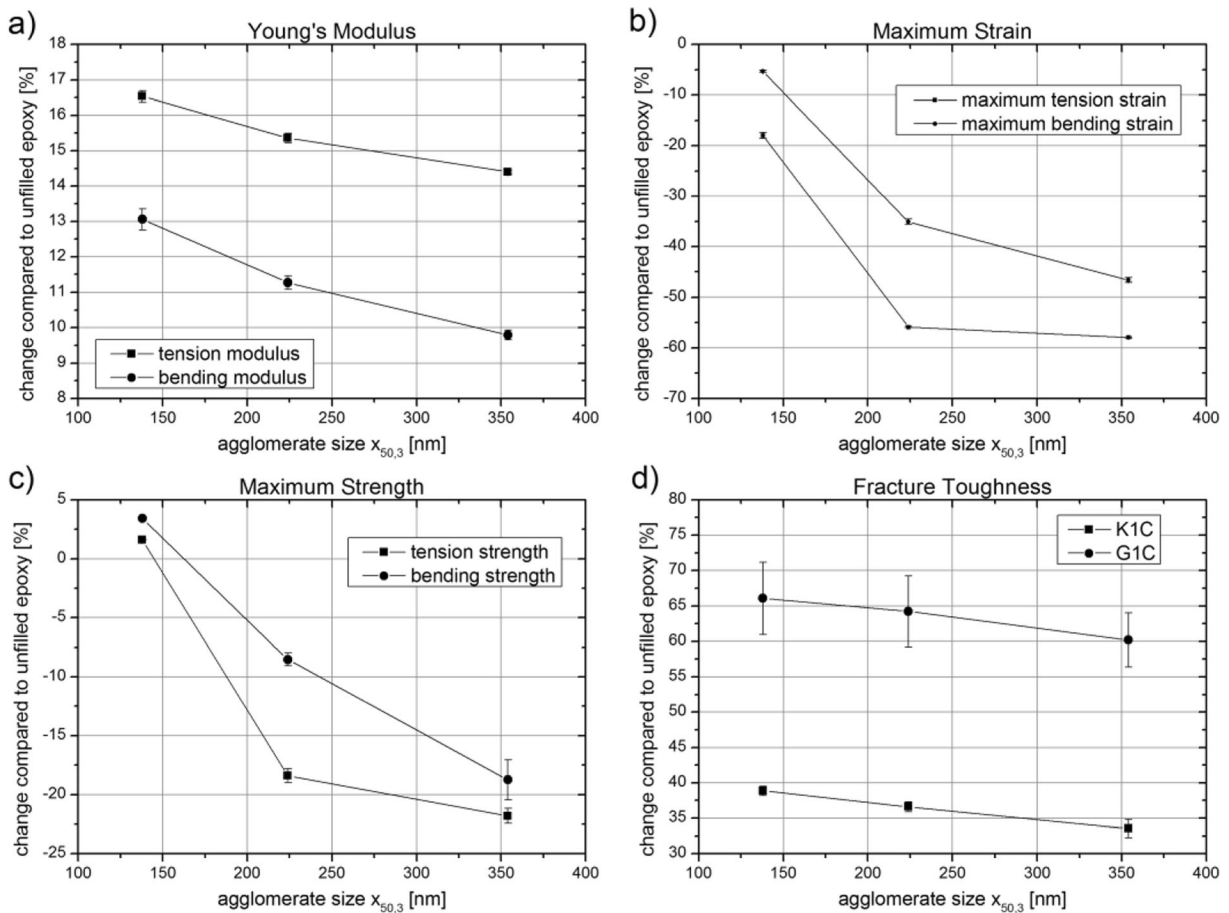


**Fig. 6** Change of mechanical properties of the nanocomposite specimen compared to the unfilled epoxy system depending on the average size of boehmite agglomerates at a constant mass fraction

of 10%. **a** Young's modulus. **b** Maximum strain. **c** Maximum strength. **d** Critical stress intensity factor  $K_{1C}$  and energy release rate  $G_{1C}$

de-bonding itself is considered to absorb only a small amount of energy. But a de-bonded particle leaves a void and thus can initiate a plastic void growth. The toughening mechanism of plastic void growth was extensively studied by Johnsen et al. (2007). They tried to predict the fracture energy with the help of the diameter of the voids. Whether their model is suited to explain the results of this study is unknown. Furthermore, Johnsen et al. used epoxy/silica composites that may have different particle-matrix interactions compared to the epoxy/boehmite composites. Nevertheless, one should consider the possibility that de-bonding and thus plastic void growth contributes to the increased fracture toughness. The fracture surfaces do not show characteristic bowing lines that indicate the mechanism of crack pinning. As it has been mentioned before, it is questionable if nanoscale particles are able to pin the crack front.

### Summary

The adjustment of the solid content in the epoxy resin was found to be a reliable method for adapting the agglomerate particle size in a kneading process, offering precise control over the product quality with deviations close to the measurement inaccuracy. This allows the production of a broad variety of agglomerate sizes with little experimental effort beforehand. Stress intensities acting during dispersion were calculated based on an approach by Rumpf and Raasch (1962). The outcome proves that dispersion results can be explained by considering the maximum stress intensity inside the kneader.

The mechanical characterization of the composite material showed an overall improvement concerning their mechanical properties. In

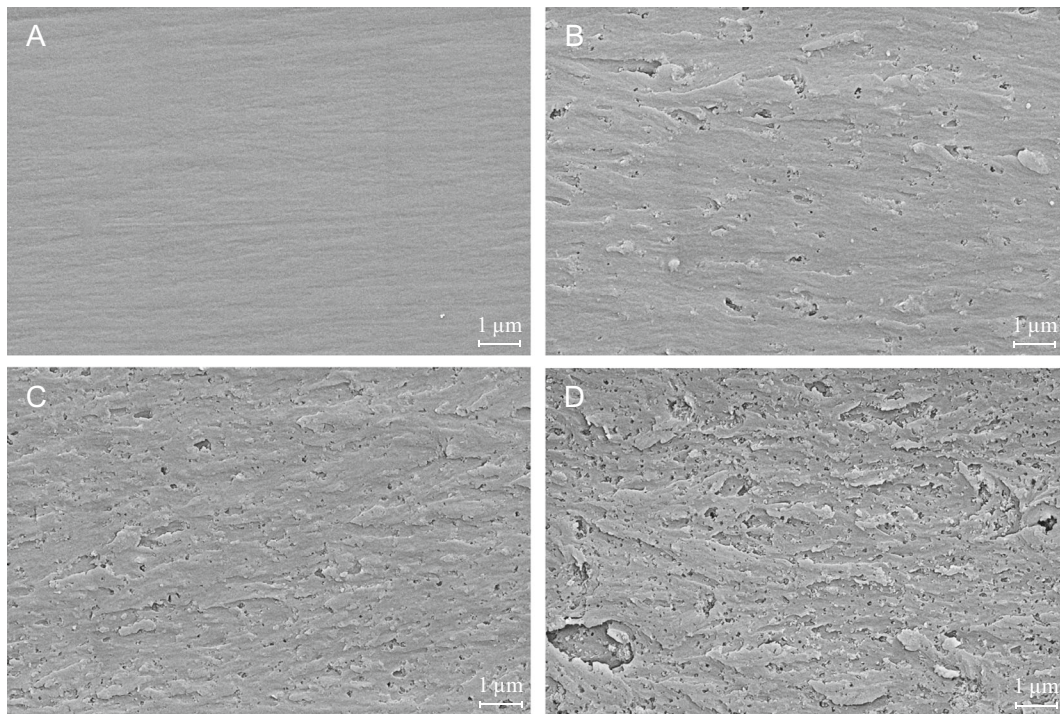


**Fig. 7** SEM pictures of the surfaces of fracture toughness samples. **a** Neat epoxy; epoxy with a mass fraction of 10 wt% boehmite and a particle size of **b** 354 nm, **c** 224 nm, and **d** 138 nm

particular, the maximum strain (40%) and the maximum strength (20%) of the composite material with an agglomerate size of 138 nm are significantly improved compared to the composite material with an agglomerate size of 354 nm. The findings suggest that larger agglomerates will break earlier and produce larger damage zones, resulting in a premature failure of the test specimen. If the maximum stress and strain can be improved any further with agglomerate sizes below 100 nm has to be confirmed in further studies. In contrast, the modulus of elasticity and the fracture toughness, which are both significantly improved by incorporation of particles in comparison to the unfilled resin, are marginally dependent on agglomerate size. Nevertheless, a statistically relevant increase between 2 and 5% was measured for both. The two main crack mechanisms that are assumed to lead to an increase in fracture toughness are crack deflection and de-bonding. The rising surface roughness and the rising content of the voids are seen as indicators for this assumption. Other mechanisms and effects like interfacial interactions and local changes in cross-link density may also be relevant and should be object of further studies. For a

comparison of the experimental and simulative tests in forthcoming studies, results concerning the elastic modulus of boehmite should be mentioned, in particular the research of Fankhänel et al. (2016). They worked with the same boehmite used in this study and found that the elastic modulus is significantly lower (~10 GPa) than reported in the literature (~80–120 GPa).

As an overall summary, it can be stated that with decreasing agglomerate sizes, the values for maximum strength and strain of the composites approximate to the values of the particle free reference. In general Young's modulus and fracture toughness can be increased significantly with particles, with only marginal influence of their agglomerates size.

**Acknowledgements** This study developed in the framework of the research unit FOR2021 "Acting Principles of Nano-Scaled Matrix Additives for Composite Structures". The authors are exceedingly grateful to the German Research Foundation (DFG) for the financial support, to Dr. Patrick Bussian (Sasol Germany GmbH) for providing the particulate material, to Peter Pfeiffer (TU Braunschweig) for the SEM pictures, and to Carmen Westphal and Marcus Kubicka for their technical support concerning the mechanical testing.

### Compliance with ethical standards

**Funding** This study was funded by the German Research Foundation (DFG).

**Conflict of interest** The authors declare that they have no conflict of interest.

### References

- Al-Turaif HA (2010) Effect of nano TiO<sub>2</sub> particle size on mechanical properties of cured epoxy resin. *Prog Org Coat* 69:241–246. doi:10.1016/j.porgcoat.2010.05.011
- Bittmann B, Hauptert F, Schlarb AK (2009) Ultrasonic dispersion of inorganic nanoparticles in epoxy resin. *Ultrason Sonochem* 16:622–628. doi:10.1016/j.ultsonch.2009.01.006
- Evans AG (1972) The strength of a brittle material containing second phase dispersions. *PHIL MAG A* 26(6):1327–1344. doi:10.1080/14786437208220346
- Exner W, Arlt C, Mahrholz T, Riedel U, Sinapius M (2012) Nanoparticles with various surface modifications as functionalized cross-linking agents for composite resin materials. *Compos Sci Technol* 72:1153–1159. doi:10.1016/j.compscitech.2012.03.024
- Faber KT, Evans AG (1983a) Crack deflection processes—I. Theory *ACTA METALL* 31(4):565–576. doi:10.1016/0001-6160(83)90046-9
- Faber KT, Evans AG (1983b) Crack deflection processes—II. Experiment *ACTA METALL* 31(4):577–584. doi:10.1016/0001-6160(83)90047-0
- Fankhänel J, Silbernagl D, Ghasem Zadeh Khorasani M et al (2016) Mechanical properties of boehmite evaluated by atomic force microscopy experiments and molecular dynamic finite element simulations. *J Nanomater* 2016(2016):1–13. doi:10.1155/2016/5017213
- Fu SY, Feng XQ, Lauke B, Mai YW (2008) Effects of particle size, particle/matrix interface adhesion and particle loading on mechanical properties of particulate–polymer composites. *COMPOS PART B-ENG* 39:933–961. doi:10.1016/j.compositesb.2008.01.002
- Green DJ, Nicholson PS, Embury JD (1979) Fracture of a brittle particulate composite. *J Mater Sci* 14:1413–1420. doi:10.1007/BF00549316
- Hall JN, Jones JW, Sachdev AK (1994) Particle size, volume fraction and matrix strength effects on fatigue behavior and particle fracture in 2124 aluminum-SiCp composites. *Mater Sci Eng A* 183:69–80
- Jamaati R, Mohammad RT, Hossein E, Mohammad RS (2014) Comparison of microparticles and nanoparticles effects on the microstructure and mechanical properties of steel-based composite and nanocomposite fabricated via accumulative roll bonding process. *MATER DESIGN* 56:359–367. doi:10.1016/j.matdes.2013.11.049
- Johnsen BB, Kinloch AJ, Mohammed RD, Taylor AC, Sprenger S (2007) Toughening mechanisms of nanoparticle-modified epoxy polymers. *Polymer* 48:530–541. doi:10.1016/j.polymer.2006.11.038
- Kinloch AJ, Mohammed RD, Taylor AC, Eger C, Sprenger S, Egan D (2005) The effect of silica nano particles and rubber particles on the toughness of multiphase thermosetting epoxy polymers. *J Mater Sci* 40:5083–5086. doi:10.1007/s10853-005-1716-2
- Kinloch AJ, Maxwell D, Young RJ (1985) Micromechanisms of crack propagation in hybrid-particulate composites. *J Mater Sci Lett* 4:1276–1279. doi:10.1007/BF00723480
- Kinloch AJ, Williams JG (1980) Crack blunting mechanisms in polymers. *J Mater Sci* 15:987–996. doi:10.1007/BF00552112
- Knieke C et al (2010) Nanoparticle production with stirred-media mills: opportunities and limits. *Chem Eng Technol* 33:1401–1411. doi:10.1002/ceat.201000105
- Lange FF, Radford KC (1971) Fracture energy of an epoxy composite system. *J Mater Sci* 6:1197–1203. doi:10.1007/BF00550091
- Lange FF (1970) The interaction of a crack front with a second-phase dispersion. *PHIL MAG A* 22(179):983–992. doi:10.1080/14786437008221068
- Nakamura Y, Yamaguchi M, Okubo M, Matsumoto T (1992) Effects of particle size on mechanical and impact properties of epoxy resin filled with spherical silica. *J Appl Polym Sci* 45:1281–1289. doi:10.1002/app.1992.070450716
- Nolte H, Schilde C, Kwade A (2012) Determination of particle size distributions and the degree of dispersion in nanocomposites. *Compos Sci Technol* 72:948–958. doi:10.1016/j.compscitech.2012.03.010
- Nolte H, Schilde C, Kwade A (2010) Production of highly loaded nanocomposites by dispersing nanoparticles in epoxy resin. *Chem Eng Technol* 33:1447–1455. doi:10.1002/ceat.201000096
- Radford KC (1971) The mechanical properties of an epoxy resin with a second phase dispersion. *J Mater Sci* 6:1286–1291. doi:10.1007/BF00552042
- Reichert H, Ruhmling K (1976) Misch- und Desagglomerationskinetik beim Kneten von Pigmentpasten. *CHEM-ING-TECH* 46:559–587. doi:10.1002/cite.330480618
- Rumpf H (1959) Beanspruchungstheorie der Prallzerkleinerung. *Chemie Ingenieur Technik* 31(5):323–337
- Rumpf H, Raasch J (1962) Desagglomeration in Strömungen. European symposium on size reduction (1st:Frankfurt a.M.: 151–159)
- Schilde C, Kampen I, Kwade A (2010) Dispersion kinetics of nano-sized particles for different dispersing machines. *Chem Eng Sci* 65:3518–3527. doi:10.1016/j.ces.2010.02.043
- Singh RP, Zhang M, Chan D (2002) Toughening of a brittle thermosetting polymer: effects of reinforcement particle size and volume fraction. *J Mater Sci* 37:781–788. doi:10.1023/A:1013844015493
- Tomo O (2008) Dispergierbare Böhmiten aus Alkoxidprozess. Science Day 2008 Nano-Techno-Science in Composite Structures and Adaptive Systems
- Wetzel B, Rosso P, Hauptert F, Friedrich K (2006) Epoxy nanocomposites—fracture and toughening mechanisms. *Eng Fract Mech* 73(16):2375–2398. doi:10.1016/j.engfracmech.2006.05.018